

Photocatalysis

International Edition: DOI: 10.1002/anie.201808177
German Edition: DOI: 10.1002/ange.201808177Pothole-rich Ultrathin WO₃ Nanosheets that Trigger N≡N Bond Activation of Nitrogen for Direct Nitrate PhotosynthesisYouwen Liu[†], Ming Cheng[†], Zhihai He, Bingchuan Gu, Chong Xiao,* Tengfei Zhou, Zaiping Guo, Jiandang Liu, Haiyan He, Bangjiao Ye, Bicao Pan, and Yi Xie*

Abstract: Nitrate is a raw ingredient for the production of fertilizer, gunpowder, and explosives. Developing an alternative approach to activate the N≡N bond of naturally abundant nitrogen to form nitrate under ambient conditions will be of importance. Herein, pothole-rich WO₃ was used to catalyse the activation of N≡N covalent triple bonds for the direct nitrate synthesis at room temperature. The pothole-rich structure endues the WO₃ nanosheet more dangling bonds and more easily excited high momentum electrons, which overcome the two major bottlenecks in N≡N bond activation, that is, poor binding of N₂ to catalytic materials and the high energy involved in this reaction. The average rate of nitrate production is as high as 1.92 mg g⁻¹ h⁻¹ under ambient conditions, without any sacrificial agent or precious-metal co-catalysts. More generally, the concepts will initiate a new pathway for triggering inert catalytic reactions.

Activating and converting inert chemical bonds directly into high value-added molecules is closely related to the quality of our lives and the health of environment.^[1–6] Thus, there is an impetus to drive chemical bond activation in various fields, ranging from industrial production to basic research. There has been success in activating the most common chemical bonds, such as C–H and C–C bonds,^[1–4] but the activation of the N≡N covalent triple bond of dinitrogen, which is essential for nitrogen fixation, is still underdeveloped.^[7–13] The high value-added nitrate products are used as a raw ingredient for the production of chemical fertilizer, gunpowder, and explo-

sives, which are of crucial importance to feed the population and defend the national security.^[14] Therefore, the industrial nitrogen fixation to nitrate, based on ammonia oxidation, followed by a multi-step chemical reaction, has been developed and employed,^[15,16] but the harsh reaction conditions (i.e. 15–25 MPa, 673–873 K, and noble metals) force scientists to seek a more moderate nitrogen fixation approach.

Photosynthesis has drawn particular attention because it relies on the photoinduced electrons and/or hole to trigger the splitting of many chemical bonds under mild conditions. To this end, various materials including diamond, BiOBr, Bi₅O₇Br, and layered-double-hydroxide have been exploited as photocatalysts to catalyse N≡N bond activation, which may provide important insights into alternative pathways for realizing nitrogen fixation.^[17–24] However, it is noteworthy that the main product of the aforementioned photocatalytic N≡N bond activation is NH₃. This only involves the first step of the industrial nitrate production process, which still requires vast additional energy consumption. Therefore, seeking more accessible approaches of N≡N bond activation for direct nitrate synthesis utilizing dinitrogen is imperative. From the perspective of the principle of chemical reactions, nitrogen fixation to nitrate is a typical oxidation reaction with increased valence of nitrogen and thus requires photogenerated holes on the valence band of a semiconductor to drive the photosynthesis of nitrate. Recently, it was discovered that TiO₂-based white paint could generate nitrate from atmospheric air under a long period of solar light irradiation due to a photocatalytic reaction. This may become useful for activating and cleaving the N≡N bond for direct nitrate synthesis under ambient conditions by semiconductor photocatalysis.^[25] Nonetheless, the barely satisfactory photocatalytic nitrate formation efficiency of nano TiO₂ limits its usage.

The catalytic activation of N₂ is extraordinarily difficult because the N≡N bond binds only weakly to solid-state catalysts, and the nonpolar N≡N covalent triple bond has high ionization energy towards dissociation.^[17,18,26,27] Focusing on the first issue, a localized electron enrichment area, which could inject considerable electrons into the empty π anti-bonding orbital of nitrogen molecules, may achieve chemisorption on solid-state catalysts.^[17] When the inorganic solids possess an uneven atomic distribution (vacancy or pothole), the charge-transfer phenomenon will occur and the electron enrichment region will subsequently emerge.^[17,28] The surface pothole structure may provide a relatively large electron enrichment area for adsorbing N₂ directly and synchronously promote the transfer of these trapped charge carriers to the adsorbates. In this regard, establishing a pothole-rich surface structure, with abundant localized electrons, could provide

[*] Dr. Y. W. Liu,^[†] M. Cheng,^[†] Z. H. He, Prof. C. Xiao, H. Y. He, Prof. B. C. Pan, Prof. Y. Xie
Hefei National Laboratory for Physical Sciences at the Microscale, CAS Centre for Excellence in Nanoscience, iCHEM, University of Science and Technology of China
Hefei, Anhui, 230026 (P. R. China)
E-mail: cxiao@ustc.edu.cn
yxie@ustc.edu.cn

Dr. B. C. Gu, Dr. J. D. Liu, Prof. B. J. Ye
State Key Laboratory of Particle Detection and Electronics, University of Science and Technology of China
Hefei, Anhui, 230026 (P. R. China)

Dr. T. F. Zhou, Prof. Z. P. Guo
Institute for Superconducting and Electronic Materials, Australian Institute for Innovative Materials (AIIM), and School of Mechanical, Materials and Mechatronics Engineering, Faculty of Engineering and Information Sciences, University of Wollongong
North Wollongong, NSW 2500 (Australia)

[†] These authors contributed equally to this work.

Supporting information and the ORCID identification number(s) for the author(s) of this article can be found under:
<https://doi.org/10.1002/anie.201808177>

a new perspective in the field of nitrate photosynthesis. Furthermore, $\text{N}\equiv\text{N}$ bond activation and conversion need extraordinarily high energy because of the high bond energy of N_2 (946 kJ mol^{-1}).^[29] For photocatalytic reactions, the photogenerated electrons and holes largely determine the reaction efficiency. The inner core electrons, which have high momentum, often get overlooked and cannot be utilized in photocatalytic reactions because they are difficult to excite under illumination. If activated, the long-neglected high momentum electrons, and the corresponding holes, could provide a stream of energy to promote the splitting of nonpolar $\text{N}\equiv\text{N}$ covalent triple bonds. The neglected issues may be solved by the design of an atomic arrangement, which may play a significant role in accelerating photocatalytic nitrogen fixation. Inspired by the aforementioned analysis, a pothole-rich surface structure, with abundant localized electrons, could be refined as a catalyst to synergistically resolve adsorption and cleavage issues during the activation of inert gas molecules.

Herein, WO_3 , which has a high redox potential,^[30] was selected as representative and realized pothole-rich WO_3 nanosheets to photocatalytically activate the $\text{N}\equiv\text{N}$ bond for direct nitrate synthesis under ambient conditions. The free-standing pothole-rich WO_3 nanosheets were constructed using a chemical topology transformation strategy,^[31] which is described in the Experimental Section in the Supporting Information. XRD and Raman spectroscopy showed the high purity of the samples (Figure S1 in the Supporting Information). The highly dense potholes with a size of about 3–4 nm on the nanosheets surfaces were clearly observed using STEM (Figure 1a and b). Furthermore, the surface percentage of the pothole area on the nanosheets is approximately 20%, based on statistical analysis of the STEM image. Furthermore, the atomic arrangement of pothole structure was directly observed in the HAADF image (Figure 1c). The HAADF image unveiled the single crystalline nature and monoclinic atomic arrangement of WO_3 nanosheets, which is consistent with the diagram of the WO_3 crystal structure viewed down the [001] zone axis (Figure 1d and e). In general, the [001] facets of the WO_3 crystal show better oxidation catalytic activity than the other facets because it possesses the highest oxygen atom density,^[30] which may be of benefit to the catalytic nitrogen fixation to nitrate. The pothole structure on the nanosheet surface is further demonstrated by the observation that the intensity of tungsten atoms gradually decreases along the superimposed red line in Figure 1c. The formation of potholes may be derived from the slight structural mismatch between WO_3 and its corresponding hydrate precursors. This special surface pothole structure is regarded as $(\text{WO}_3)_n$ voids, which provide additional dangling bonds relative to the single vacancy for the direct bridging/adsorbing of N_2 . The thickness of nanosheets was measured quantitatively, using AFM, (Figure 1f and g) to be about 3.5 nm, which is close to five unit-cell monoclinic WO_3 atomic layers. The ultrathin configuration of these nanosheets ensures a high surface pothole percentage. These characterizations show that pothole-rich WO_3 nanosheets, with a high-activity exposed lattice plane, were successfully prepared.

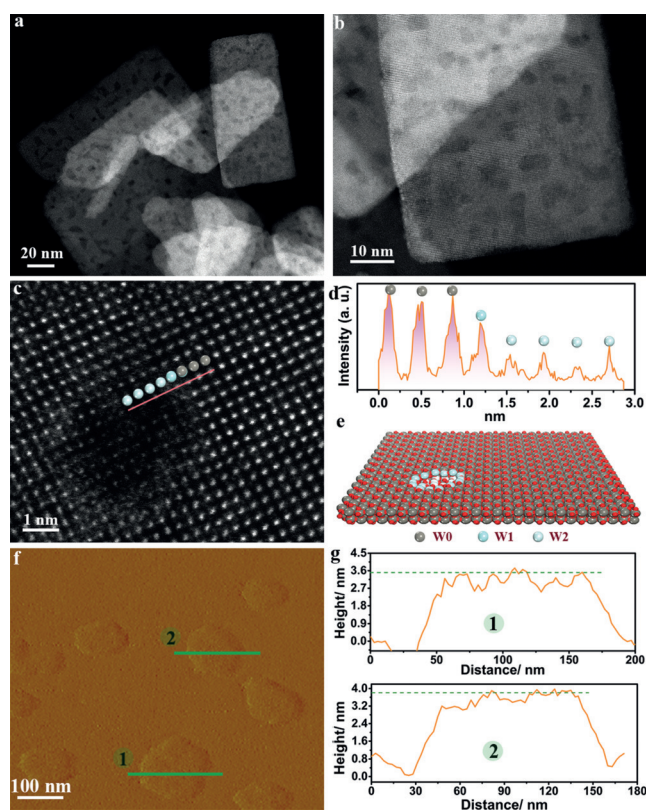


Figure 1. Structural characterization of pothole-rich WO_3 nanosheet. a, b) Representative STEM image. c, d) Atomic-resolution HAADF-STEM image. e) Illustration of pothole-rich WO_3 nanosheet. W0, W1 and W2 stand for tungsten atoms of pothole-free area, surrounding pothole, pothole area, respectively. f, g) Atomic force microscopy (AFM) image and the corresponding height profiles.

To evaluate the performance of this material as a photocatalyst for nitrate formation, pothole-rich WO_3 nanosheets and control samples were dispersed in water and the produced nitrate was detected using high-performance ion chromatography (HPIC). The experimental information is detailed in the Methods section in the Supporting Information. In the photoreactor under 300 W Xe lamp irradiation, the nitrate concentration increased almost linearly with the reaction time when purified mixed gas ($V_{\text{N}_2}:V_{\text{O}_2} = 3:1$) was purged into the reactor. The yield of NO_3^- could be almost 5.77 mg g^{-1} after 3 h with an average nitrate-producing rate of $1.92 \text{ mg g}^{-1} \text{ h}^{-1}$ (Supporting Information, Figures S2, S3, and Table S1), which is almost 9.8 and 16.5 times that obtained when using pothole-free WO_3 nanosheets and bulk WO_3 (Supporting Information, Figure S4), respectively. Furthermore, the pothole-rich WO_3 nanosheets exhibit outstanding stability with no obvious attenuation in activity observed after ten successive photocatalytic cycles (Figure 2b). The negligible morphological evolution after ten successive photocatalytic cycles, as observed using TEM, also suggests good structural stability because the potholes are still visible (Supporting Information, Figure S5). Furthermore, a control experiment indicated that there was no detectable nitrate generation in the absence of nitrogen, confirming that the nitrate product is derived from the N_2 reaction on the

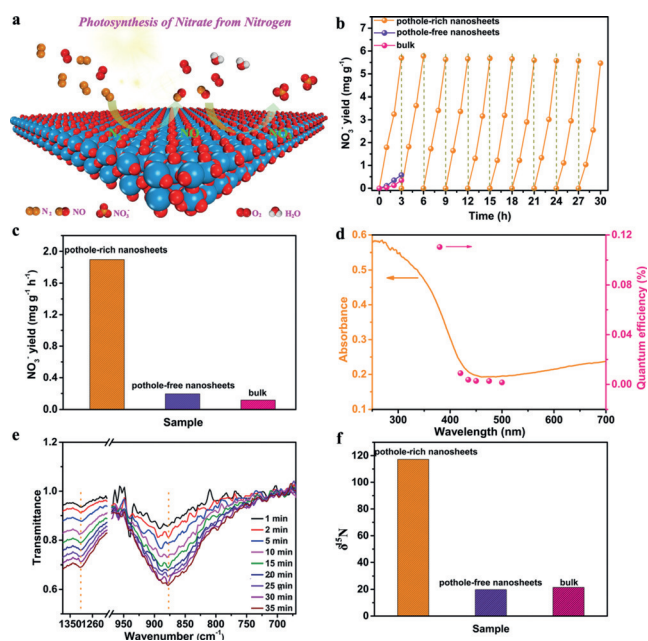
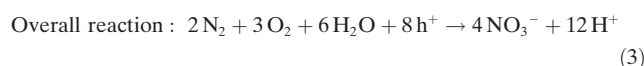
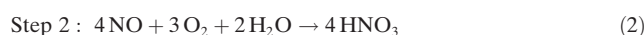


Figure 2. Photocatalytic nitrate formation from nitrogen and oxygen. a) Schematic illustration of photoconversion of N₂ into nitrate at ambient conditions. b) Concentration profiles of nitrate. c) Nitrate formation rate calculated by the nitrate concentration profiles. d) The wavelength-dependent apparent quantum efficiency under monochromatic light irradiation. e) In situ synchrotron radiation FTIR differential spectrum. f) The testing concentration of ¹⁵N element by Stable Isotope Ratio Mass Spectrometer.

photocatalyst (Supporting Information, Figure S6). The apparent quantum efficiency (AQE) decreased as the wavelength of the monochromatic light increased. Under UV/Vis irradiation at 380 nm, the AQE was calculated to be 0.11%, which is about 2.3 and 4.5 times that of the pothole-free nanosheets and bulk WO₃, respectively (Figure 2d; Supporting Information, S7 and Table S2). Moreover, to gain further insight into the photocatalytic nitrate formation process, in situ synchrotron radiation Fourier transform infrared spectroscopy (FTIR) measurements were performed for three samples (Figure 2e and Supporting Information, Figure S8). For pothole-rich WO₃ nanosheets, two characteristic peaks at 875 cm⁻¹ and 1305 cm⁻¹ were observed and they gradually increased with increasing irradiation time. These peaks could be attributed to the internal bending vibration absorption peak and asymmetric stretching vibration absorption peak of nitrate, respectively. In contrast, no significant change was observed in the FTIR spectra of pothole-free WO₃ nanosheets and bulk WO₃. The time-dependent in situ tests further confirmed that nitrate was formed directly from dissociative nitrogen molecules, under ambient conditions, over the constructed pothole-rich nanosheets. To provide further evidence regarding the origin of the nitrate generated from N₂ activation, an isotopic labeling experiment using ¹⁵N₂ as the purge gas was conducted. The obtained ¹⁵NO₃⁻ was measured using stable isotope-ratio mass spectrometry. The testing concentration of ¹⁵N was evaluated by the parameter δ¹⁵N ($\delta^{15}\text{N} = \frac{C_{\text{sample}}^{15\text{N}}}{C_{\text{standard}}^{15\text{N}}} - 1$). As seen in Figure 2f, all products outclass the corresponding standard abundance, and

the value of δ¹⁵N in pothole-rich WO₃ nanosheets is much larger than that obtained using contrastive photocatalysts. These isotopic labeling results clearly confirm that the N element of the generated nitrate came from N₂.

The critical concern of photocatalytic nitrogen fixation is how to adsorb and activate the N≡N bond of N₂ molecules. To investigate the catalytic mechanism for pothole-rich nanosheets on the molecular level, density functional theory (DFT) calculations were conducted. First, possible intermediates and reaction channels for direct nitrate synthesis over pothole-rich WO₃ were screened. Based on the finding that the electron acceptor, methyl viologen dichloride, could significantly improve the nitrogen fixation efficiency of constructed catalysts (Supporting Information, Figure S9), the nitrogen fixation process was determined to follow the photogenerated-hole oxidation mechanism, following these two steps:



The proposed mechanism indicates that photogenerated-hole oxidation involves multiple steps and considerable barriers,^[25] which are not conducive to trigger nitrogen fixation favorably. This conclusion could also be drawn in this catalytic system, based on the DFT simulation. The free energy profile and the reaction pathway of nitrate synthesis on pothole-free WO₃ are depicted in Figure 3a, b. From the charge density difference (Supporting Information, Figure S10), the nitrogen molecules cannot be adsorbed on the pothole-free WO₃ surface directly. Therefore, the formation of anchor sites on pothole-free WO₃ must require the two-step adsorption of H₂O and the four-step desorption of hydrogen atom. Furthermore, the specific Gibbs reaction energy (ΔG) of all steps was simulated. As shown Figure 3b, all transformation reaction steps (such as formation of reaction state D-G) involve a high energy barrier of above 1.0 eV, reaching up to -2.17 eV for the dissociation of molecular NO step. The considerable Gibbs reaction energy makes the nitrogen adsorption process and nitrogen fixation in pothole-free WO₃ considerably difficult. The abundant dangling bonds of the pothole-rich WO₃ nanosheets could provide sites to anchor N₂ and may realize nitrogen adsorption and catalysis directly. As such, the obvious charge-transfer behavior (reaction state A in Figure 3c) between the pothole-rich site and N₂ suggests the strong chemisorption behavior of N₂ and the pothole-rich surface, which may derive from the electron enrichment of the dangling oxygen atoms. In this step, the Gibbs reaction energy is 0.71 eV, and the formed adsorbed state (reaction state B in Figure 3c) is considered as a metastable intermediate state. In the following step, N≡N bonds of nitrogen molecules adsorbed on pothole-rich WO₃ nanosheets will be easily activated and converted into N–N bonds in the form of NO, with an energy barrier of -0.91 eV. The next step, NO could naturally

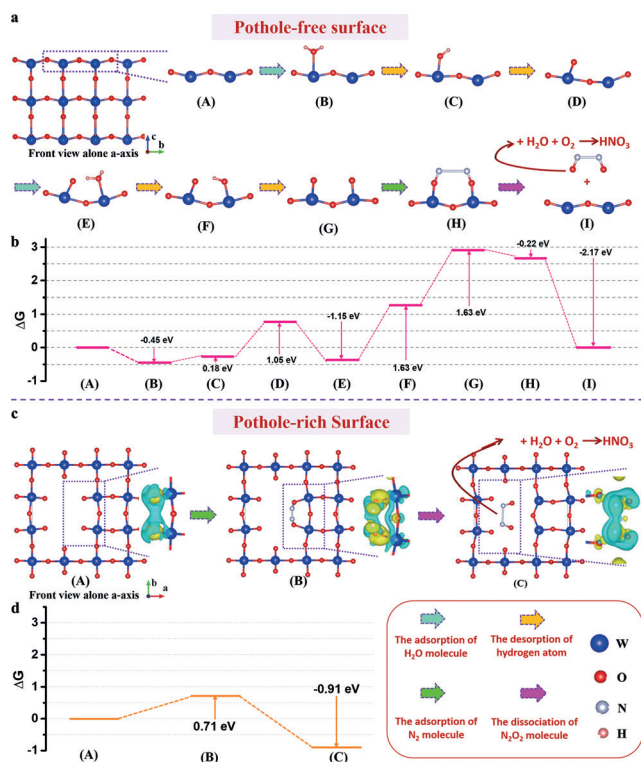


Figure 3. The activation and cleavage of N≡N bonds of N₂ for direct nitrate synthesis. a) The multistep process in pothole-free WO₃. b) Calculated Gibbs free energy diagram of reaction transformation process over pothole-free WO₃. c) According to the DFT calculation, the dangling bonds of the pothole area play a critical role in adsorbing the molecular state of nitrogen and the intermediate state (B) is metastable, which could strip out the molecular N₂O₂ as the precursor of nitrate. d) The specific Gibbs free energy diagram of the stepwise of activation and cleavage of N≡N bonds of N₂.

translate into nitrate with O₂ and H₂O. Therefore, the peculiar atomic arrangement of pothole-rich WO₃ nanosheets enables photocatalytic nitrogen fixation to occur via a direct reaction pathway.

Notably, to maintain the catalytic reaction (Supporting Information, Figure S11), the reactive state D could be replenished by foreign oxygen atoms from adsorbing H₂O molecules and desorbing hydrogen atoms. The reactive state D possesses strong adsorption ability for H₂O molecules, with an adsorption energy of -2.88 eV, determined by theoretical simulation calculations. Furthermore, for the desorption of hydrogen, the hydrogen atoms could smoothly migrate along the surrounding oxygen atoms. The energy barrier of hydrogen migration was calculated as 0.02 eV. Overall, the energy barrier of hydrogen migration ranges between 0.11 eV and 0.16 eV, showing that the hydrogen atoms could migrate over the catalytic surface. In summary, the N₂ molecules could directly adsorb on the dangling bonds of pothole-rich WO₃ nanosheets and form the metastable reactive state B. The adsorbed N₂ molecules could then be easily activated and converted into NO. Adsorption sites could be replenished by foreign oxygen atoms from adsorbing H₂O molecules.

The information of confined electrons is a directive for evaluating the efficiency of photocatalysis. In this regard,

positron annihilation spectroscopy was carried out to explore the electron information, including that of inner core electrons namely high momentum electrons. The W parameter of the Doppler broadening spectrum is an immediate parameter for evaluating the high momentum electrons of catalysts. The larger the W parameter the easier the high momentum electrons could be excited into the valence shell. In this work, the W parameters were acquired from the Doppler broadening spectrum of annihilation radiations (Figure 4a) in the $(-33.5--8) \times 10^{-3} m_0 c$ and $(7-32.5) \times 10^{-3} m_0 c$ section. The W parameters for pothole-rich WO₃

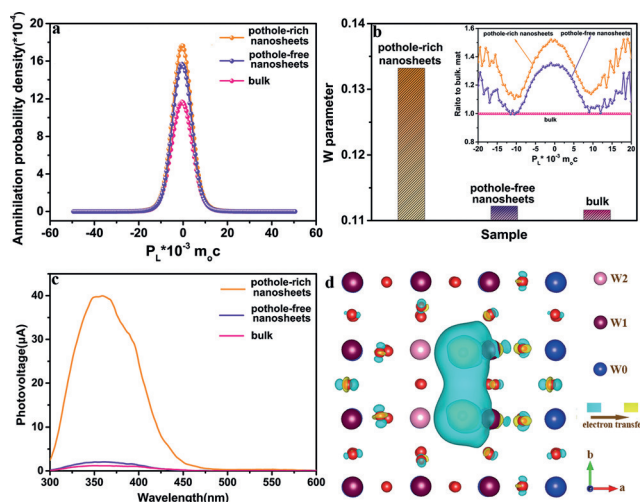


Figure 4. The information of electronic structure. a) Doppler spectra of catalysts. b) The contrast of the W parameter. Inset: The ratio of the experimental positron-electron momentum distribution to the positron-electron momentum distribution of bulk WO₃. c) Surface photovoltage spectrum. d) The charge difference density of the pothole-rich WO₃ nanosheet around the pothole region.

nanosheet, pothole-free WO₃ nanosheets, and bulk WO₃ were 0.1332, 0.1122, and 0.1116, respectively, which indicates that it was easier to excite the high momentum electrons in the inner core into the valence shell in pothole-rich WO₃ nanosheets. The distinctive electron movement characteristic may derive from the pothole atomic arrangement. Therefore, the electron distribution of pothole-rich WO₃ nanosheets was inspected and simulated by DFT. Based on the isosurfaces of electron density differences, a visible electron transferring phenomenon from the W1 atom to the dangling oxygen atom could be observed around the pothole region. In other words, the dangling oxygen atoms spontaneously form an electron enrichment area. The atomic arrangement and induced electron distribution may play a key role in stimulating inner high momentum electrons to participate in the photocatalytic nitrogen fixation process. Furthermore, an order of magnitude increase of surface photovoltage for pothole-rich WO₃ nanosheets relative to the reference samples could demonstrate that the high momentum electrons were excited (Figure 4c). More easily excited high momentum electrons of pothole-rich nanosheets provide more photogenerated holes to accelerate the activation of nonpolar N≡N covalent triple

bonds, and thus promote direct nitrate photosynthesis efficiency.

Integrating all experiments, the N≡N covalent triple bond of N₂ molecules could be activated and converted into nitrate under ambient conditions using green photocatalysis technology. Combined with the theoretical simulation, the pothole-rich structure could provide abundant anchor sites for the direct adsorption, and subsequent activation, of N₂ molecules. These findings show that invoking high momentum electrons to participate in photocatalysis accelerates the activation and cleavage of N≡N covalent triple bonds. This strategy also provides an important insight into many other photo-induced chemical bond activations for photocatalytic reactions, such as CO₂ reduction and water splitting, due to their shared origin. Furthermore, we note that photocatalytic nitrate-synthesizing directly using N₂ molecules emerge glaring prospects although the throughput is no match for its industrial process. Therefore, further efforts are devoted to improving the efficiency of nitrate production to reach the demand of large-scale industrial production.

Acknowledgements

This work was financially supported by the National Key R&D Program of China (2017YFA0207301), the National Natural Science Foundation of China (21622107, U1832142, 11621063 and U1532265), the Youth Innovation Promotion Association CAS (2016392), the Key Research Program of Frontier Sciences (QYZDY-SSW-SLH011), the Fundamental Research Funds for the Central University (WK2340000075), and the Major Program of Development Foundation of the Hefei Center for Physical Science and Technology (2017FXZY003). The computational center of USTC is acknowledged for computational support.

Conflict of interest

The authors declare no conflict of interest.

Keywords: chemical bond activation · high momentum electrons · nitrate photosynthesis · pothole-rich nanosheets · WO₃

How to cite: *Angew. Chem. Int. Ed.* **2019**, *58*, 731–735
Angew. Chem. **2019**, *131*, 741–745

- [1] Y. Xia, G. Lu, P. Liu, G. B. Dong, *Nature* **2016**, *539*, 546–550.
[2] A. Masarwa, D. Didier, T. Zabrodski, M. Schinkel, L. Ackermann, I. Marek, *Nature* **2014**, *505*, 199–203.
[3] Z. Zhang, K. Tanaka, J. Yu, *Nature* **2017**, *543*, 538–542.

- [4] A. McNally, B. Haffemayer, B. S. Collins, M. J. Gaunt, *Nature* **2014**, *510*, 129–133.
[5] L. Hie, N. F. F. Nathel, T. K. Shah, E. L. Baker, X. Hong, Y. F. Yang, P. Liu, K. N. Houk, N. K. Garg, *Nature* **2015**, *524*, 79–83.
[6] S. J. Blanksby, G. B. Ellison, *Acc. Chem. Res.* **2003**, *36*, 255–263.
[7] J. W. Erisman, M. A. Sutton, J. Galloway, Z. Klimont, W. Winiwarter, *Nat. Geosci.* **2008**, *1*, 636–639.
[8] J. S. Anderson, J. Rittle, J. C. Peters, *Nature* **2013**, *501*, 84–88.
[9] K. Arashiba, Y. Miyake, Y. Nishibayashi, *Nat. Chem.* **2011**, *3*, 120–125.
[10] D. V. Yandulov, R. R. Schrock, *Science* **2003**, *301*, 76–78.
[11] S. Licht, B. Cui, B. Wang, F. F. Li, J. Lau, S. Liu, *Science* **2014**, *345*, 637–640.
[12] G. J. Leigh, *Science* **1998**, *279*, 506–507.
[13] D. E. Canfield, A. N. Glazer, P. G. Falkowski, *Science* **2010**, *330*, 192–196.
[14] A. J. Medford, M. C. Hatzell, *ACS Catal.* **2017**, *7*, 2624–2643.
[15] G. Ertl, *Catal. Rev. Sci. Eng.* **1980**, *21*, 201–223.
[16] T. Rayment, R. Schlogl, J. M. Thomas, G. Ertl, *Nature* **1985**, *315*, 311–313.
[17] H. Li, J. Shang, Z. Ai, L. Zhang, *J. Am. Chem. Soc.* **2015**, *137*, 6393–6399.
[18] D. Zhu, L. Zhang, R. E. Ruther, R. J. Hamers, *Nat. Mater.* **2013**, *12*, 836–841.
[19] S. Wang, X. Hai, X. Ding, K. Chang, Y. Xiang, X. Meng, Z. Yang, H. Chen, J. Ye, *Adv. Mater.* **2017**, *29*, 1701774.
[20] Y. Zhao, Y. Zhao, G. I. N. Waterhouse, L. Zheng, X. Cao, F. Teng, L. Wu, C.-H. Tung, D. O'Hare, T. Zhang, *Adv. Mater.* **2017**, *29*, 1703828.
[21] C. Li, T. Wang, T.-J. Zhao, W. Yang, J.-F. Li, A. Li, Z. Z. Yang, G. Ozin, J. Gong, *Angew. Chem. Int. Ed.* **2018**, *57*, 5278–5522; *Angew. Chem.* **2018**, *130*, 5376–5380.
[22] R. I. Bickley, V. Vishwanathan, *Nature* **1979**, *280*, 306–308.
[23] O. Linnik, H. Kisch, *Photochem. Photobiol. Sci.* **2006**, *5*, 938–942.
[24] O. Rusina, O. Linnik, A. Eremanko, H. Kisch, *Chem. Eur. J.* **2003**, *9*, 561–565.
[25] S. J. Yuan, J. J. Chen, Z. Q. Lin, W. W. Li, G. P. Sheng, H. Q. Yu, *Nat. Commun.* **2013**, *4*, 2249.
[26] G. N. Schrauzer, T. D. Guth, *J. Am. Chem. Soc.* **1977**, *99*, 7189–7193.
[27] M. Vettraino, M. Trudeau, A. Y. Lo, R. W. Schurko, D. Antonelli, *J. Am. Chem. Soc.* **2002**, *124*, 9567–9573.
[28] Y. Liu, T. Zhou, Y. Zheng, Z. He, C. Xiao, W. K. Pang, W. Tong, Y. Zou, B. Pan, Z. Guo, Y. Xie, *ACS Nano* **2017**, *11*, 8519–8526.
[29] J. Itatani, J. Levesque, D. Zeidler, H. Niiikura, H. Pépin, J. C. Kieffer, P. B. Corkum, D. M. Villeneuve, *Nature* **2004**, *432*, 867–871.
[30] H. Jin, J. Zhu, W. Chen, Z. Fang, Y. Li, Y. Zhang, X. Huang, K. Ding, L. Ning, W. Chen, *J. Phys. Chem. C* **2012**, *116*, 5067–5075.
[31] Y. Liu, L. Liang, C. Xiao, X. Hua, Z. Li, B. Pan, Y. Xie, *Adv. Energy Mater.* **2016**, *6*, 1600437.

Manuscript received: July 17, 2018

Revised manuscript received: November 20, 2018

Accepted manuscript online: November 22, 2018

Version of record online: December 13, 2018